JMEPEG (2015) 24:2556–2562
DOI: 10.1007/s11665-015-1527-9

1059-9495/$19.00

Effect of Metal Matrix Alloying on Mechanical Strength of Diamond Particle-Reinforced Aluminum Composites

Hailong Zhang, Jianhua Wu, Yang Zhang, Jianwei Li, and Xitao Wang

(Submitted December 16, 2014; in revised form April 8, 2015; published online April 24, 2015)

Diamond particle-reinforced Al matrix (Al/diamond) composites were produced by a gas pressure infiltration method, where 0.5-4.0 wt.% Ti was added to Al matrix. An interfacial TiC layer of about 2 μm thickness was formed between Al and diamond at 4.0 wt.% Ti addition. The mechanical properties of the Al/diamond composites were enhanced by both the formation of interfacial layer and the strengthening of the matrix. The mechanical strength increased with increasing alloying Ti content, and a tensile strength of 153 MPa was obtained at 4.0 wt.% Ti addition. The tensile flow stress of the composites was found to be in broad agreement with the prediction of the Mori-Tanaka model. The effect of interfacial layer on mechanical properties provides guideline for the production of mechanically reliable Al/diamond composites.

Keywords casting and solidification, mechanical properties, metal matrix composites

1. Introduction

With the highly integration of electronic devices, the assemblies are demanding heat-spreading materials with high thermal conductivity (TC) (Ref 1, 2). Traditional packaging materials such as W-Cu, AlN, SiC, and Al/SiC cannot meet such a technical challenge (Ref 3). Diamond possesses the highest TC (1200-2000 W/mK) among natural materials; however, its coefficient of thermal expansion (CTE, 1-2 ppm/K) is not compatible with that of semiconductors (4-6 ppm/K). Since metals like Cu and Al exhibit both high TC and relatively large CTE, the combination of diamond and metals could give rise to both high TC (Ref 4, 5) and tailorable CTE in diamond particle-reinforced metal matrix (metal/diamond) composites. Furthermore, metal matrix endows such composites with excellent formability and machinability. Recently, Al/diamond composites are reported to have TC with a level of >700 W/mK (Ref 6) that is much higher than other electronic packaging materials.

During machining, assembly, and service of Al/diamond composites, considerable mechanical stresses are inevitably incurred. Electronic packaging applications are appealing for an acceptable comprehensive performance from thermal conducting composites. While the thermal conductivity has been extensively investigated, the mechanical behavior of Al/diamond composites is rarely reported. Weidenmann et al. (Ref 7, 8) surveyed the Young' modulus, mechanical strength, and fracture toughness of several sorts of composites like Al-Cu/diamond, Cu-B/diamond, and Ag-Si/diamond. For the Al/diamond composites concerned, they presented the effects of diamond volume fraction and diamond particle size on mechanical properties of the composites. Since they dealt with just one composition of Al-2.0 wt.% Cu matrix, the effect of alloying Cu content on mechanical properties of Al/diamond composites remains unclear.

The addition of alloying element to Al matrix is to enhance interfacial bonding by the formation of interfacial carbide layer, since large wetting angle occurs between diamond and Al. It is well known that Ti acts as a strong carbide-forming element. While the effect of Ti addition to Al matrix on thermal conductivity of Al/diamond composites has been manifested (Ref 9-12), the effect of Ti addition on the mechanical behavior is still unknown. Furthermore, the interfacial carbide layer guarantees load transfer from metal matrix to diamond reinforcement. The interfacial layer thickness is thus critical to strengthen the load transfer. By designing and generating a series of interfacial layers with varied thickness, the role of interfacial carbide layer in enhancing the mechanical strength of Al/diamond composites can be demonstrated. So far, the issue has not been solved.

In this study, a series of Ti contents are alloyed to Al matrix to achieve various thicknesses of interfacial TiC layer between diamond and Al. The effect of interfacial layer thickness on mechanical properties of Al-Ti/diamond composites is thus clarified. Then, the Mori-Tanaka model is applied to correlate the tensile stress-strain curves of the composites.

2. Experimental

2.1 Materials

Table 1 gives the starting materials used in the experiments. The as-received diamond powders were cleaned in a 10 vol.% HCl and 90 vol.% H_2O solution for 30 min to remove impurity. For metal matrix alloying, the Al bulks were melted with the Al-4.0 wt.% Ti bulks to obtain Al-xTi alloys (x = 0, 0.5, 1.0, 2.0, 3.0, 4.0 wt.%) by a vacuum-induction melting.

Hailong Zhang, Yang Zhang, Jianwei Li, and **Xitao Wang**, State Key Laboratory for Advanced Metals and Materials, University of Science and Technology Beijing, Beijing 100083, China; and **Jianhua Wu**, State Key Laboratory for Advanced Metals and Materials, University of Science and Technology Beijing, Beijing 100083, China; and Institute of New Materials, Shandong Academy of Sciences, Jinan 250014, China. Contact e-mail: xtwang@ustb.edu.cn.

Table 1 Starting materials used in the experiments

Material	Type	Purity	Average particle size	Source
Diamond	MBD-4	…	80/100 mesh, 159 μm	Luoyang Diamond
Al	…	99.99%	Bulks	Beijing Cuibolin Non-ferrous
Al-4.0 wt.% Ti	…	…	Bulks	New Metal Materials, Hebei Sitong

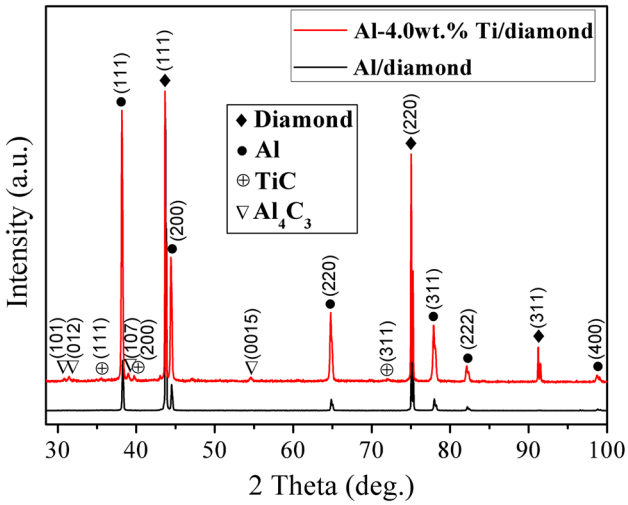

Fig. 1 XRD patterns of the Al-Ti/diamond composites produced by gas pressure infiltration

2.2 Infiltration

The Al/diamond composites were produced by a gas pressure infiltration method. The diamond powders were installed into a graphite mold, with Al or Al-Ti bulks covering on top of the diamond particles bed. The assembly was then moved to a chamber for infiltration. The chamber was evacuated to a vacuum below 0.1 Pa, before heating to infiltration temperature with a ramp rate of 50 K/min. When the predefined infiltration temperature was achieved, high-purity argon gas was pumped into the chamber to maintain a gas pressure of 1.0 MPa. The infiltration was kept for 20 min at the infiltration temperature. Then, the heating power was switched off and the samples were furnace cooled down to room temperature. The infiltration temperature was 1073 K for unalloyed Al matrix composite. Since Ti alloying increases the melting point of the resultant Al-Ti alloys, the infiltration temperature was raised from 1073 to 1253 K, corresponding to alloyed Ti content from 0 to 4.0 wt.%. The composites produced with Ti-alloyed Al matrix are hereafter recognized as Al-Ti/diamond composites.

2.3 Mechanical Testing

The mechanical testing for the produced Al-Ti/diamond composites includes tensile, compressive, and bending loadings, which were conducted on a material testing platform (MTS 809, MTS Systems Corporation, USA). The tensile loading rate was 0.5 mm/min, using plate specimens 3 mm in thickness with a gage size of 4 mm × 15 mm. The compressive strain rate was 1×10^{-3} s^{-1}, using specimens with dimensions of 3 mm × 3 mm × 8 mm. The bending loading rate was 0.3 mm/min, using specimens with dimensions of 3 mm × 5 mm × 30 mm. At least three specimens were used for each testing. The mechanical strength was derived on the average of three tests, and the error was thus determined.

2.4 Characterization

The phase structure of the Al-Ti/diamond composites was characterized by x-ray diffraction (XRD, Rigaku DMAX-RB, Japan). In order for microstructural observation, the samples were polished using a diamond-containing grinding machine. The polished surface was then observed using backscattered electron pattern in scanning electron microscope (SEM, ZeissSupra55, Germany). The interparticle distance between dispersed diamond particles was determined upon several polished surfaces using the intercept method, giving an error of about ±5 μm. After mechanical testing, the fractured surfaces of Al-Ti/diamond composites were also characterized by SEM.

3. Results

3.1 Microstructure

Figure 1 shows the XRD patterns of the produced Al-Ti/diamond composites. For the unmodified Al/diamond composite, only Al (PDF# 85-1327) and diamond (PDF# 79-1467) phases were detected. For the Al-4.0 wt.% Ti/diamond composite, however, both TiC (PDF# 71-0298) and Al_4C_3 (PDF# 35-0799) were additionally observed. The presence of TiC comes from the interfacial reaction between alloyed Ti and diamond. The formation of Al_4C_3 is owing to the interfacial reaction between Al matrix and diamond during infiltration. Since the reaction varies kinetically when the composites are processed at different temperatures (Ref 13), Al_4C_3 was detected in the Al-4.0 wt.% Ti/diamond composite at the high infiltration temperature of 1253 K.

Figure 2 shows the backscattered electron images (BEI) of the Al-Ti/diamond composites. The diamond particles were uniformly dispersed in the Al matrix, and they had a narrow distribution of particle size (Fig. 2a and b). The metallographic examination shows that the loading of diamond particles was about 65 vol.%, higher than 60 vol.% obtained by squeeze casting (Ref 14). From Fig. 2(a), the interparticle distance was determined to be about 168 μm, a bit larger than the average particle size of 159 μm. This suggests that the diamond particles are separated by a very thin layer of Al matrix. As shown from Fig. 2(c-f), there was a distinct interface between diamond reinforcement and Al matrix. Since the interfacial layer has a limited thickness, it cannot be directly observed from the BEI photos.

In order to examine the interfacial layer between diamond and Al, x-ray mapping analysis was performed on the Al-4.0 wt.% Ti/diamond composite, as shown in Fig. 3. The Ti dissolved in Al matrix as well as accumulated at the interface can be clearly seen from the x-ray mapping. The line scan

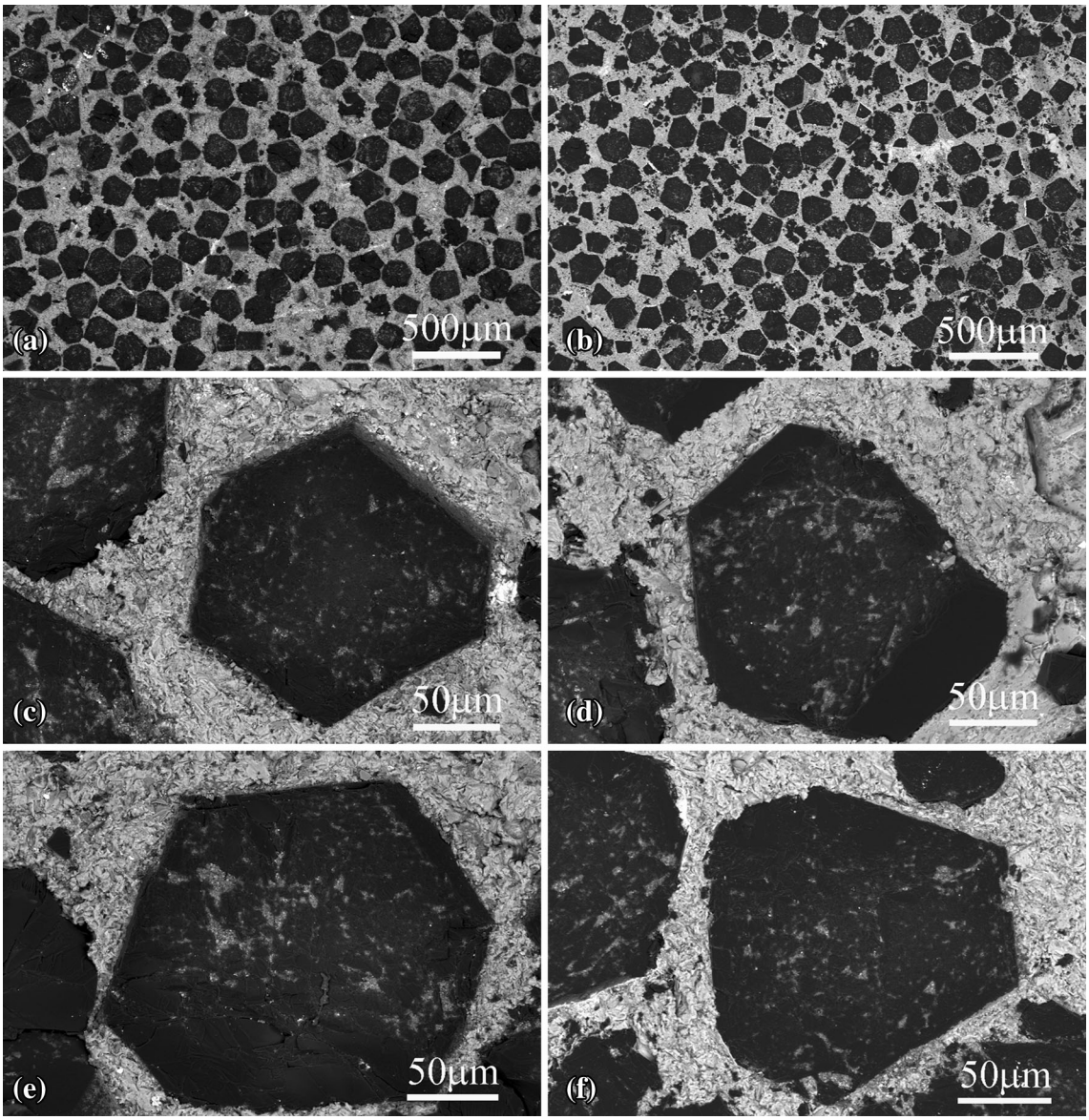

Fig. 2 SEM observations of polished surfaces of the produced Al-*x*Ti/diamond composites: (a) x = 0 wt.% and (b) x = 4.0 wt.% (at low magnification), and (c) x = 0 wt.%, (d) x = 0.5 wt.%, (e) x = 2.0 wt.%, and (f) x = 4.0 wt.% (at high magnification)

shows that the transition zone between Al and diamond had a width of about 2 μm. It is reasonably deduced that some of the dissolved Ti has reacted with diamond to form TiC, which is verified by the XRD results in Fig. 1.

3.2 Mechanical Properties

3.2.1 Tensile Strength. Figure 4 shows the representative tensile stress-strain curves of the Al-Ti/diamond composites. As summarized in Table 2, the ultimate tensile strength (UTS) monotonically increased up to 4.0 wt.% Ti. Compared with the unmodified Al/diamond composite, the formation of interfacial layer promotes the bonding between diamond reinforcement and Al matrix and thus raises the tensile strength. The strain at failure firstly decreased to 0.5 wt.% Ti and then gradually increased up to 4.0 wt.% Ti, recovering to the level of the unmodified Al/diamond composite.

Since there is no distinct linear elastic regime in the tensile curves, the determination of a true yield point is almost impossible. According to Kouzeli and Mortensen's process (Ref 15), we define $\sigma_{0.02\%}$ and $\sigma_{0.2\%}$, the 0.02 and 0.2% offset stresses, respectively, as yield stresses of Al/diamond composites. Table 2 shows the determination of $\sigma_{0.02\%}$ and $\sigma_{0.2\%}$ for the Al-Ti/diamond composites. It can be seen that the $\sigma_{0.02\%}$ value monotonically increased with increasing Ti content, which is rationalized by alloy strengthening effect. As for the indicator of $\sigma_{0.2\%}$, which is often used to define the onset of plastic deformation in metals, it is deeply influenced by tensile strain hardening and cannot represent a true measure of yield. The $\sigma_{0.2\%}$ values for 0.5 and 2.0 wt.% Ti are not available due to their limited plastic strains.

Young's modulus (E_0) of the Al-Ti/diamond composites can be determined from the tensile stress-strain curves. The determination of E_0 should employ the initial stage of

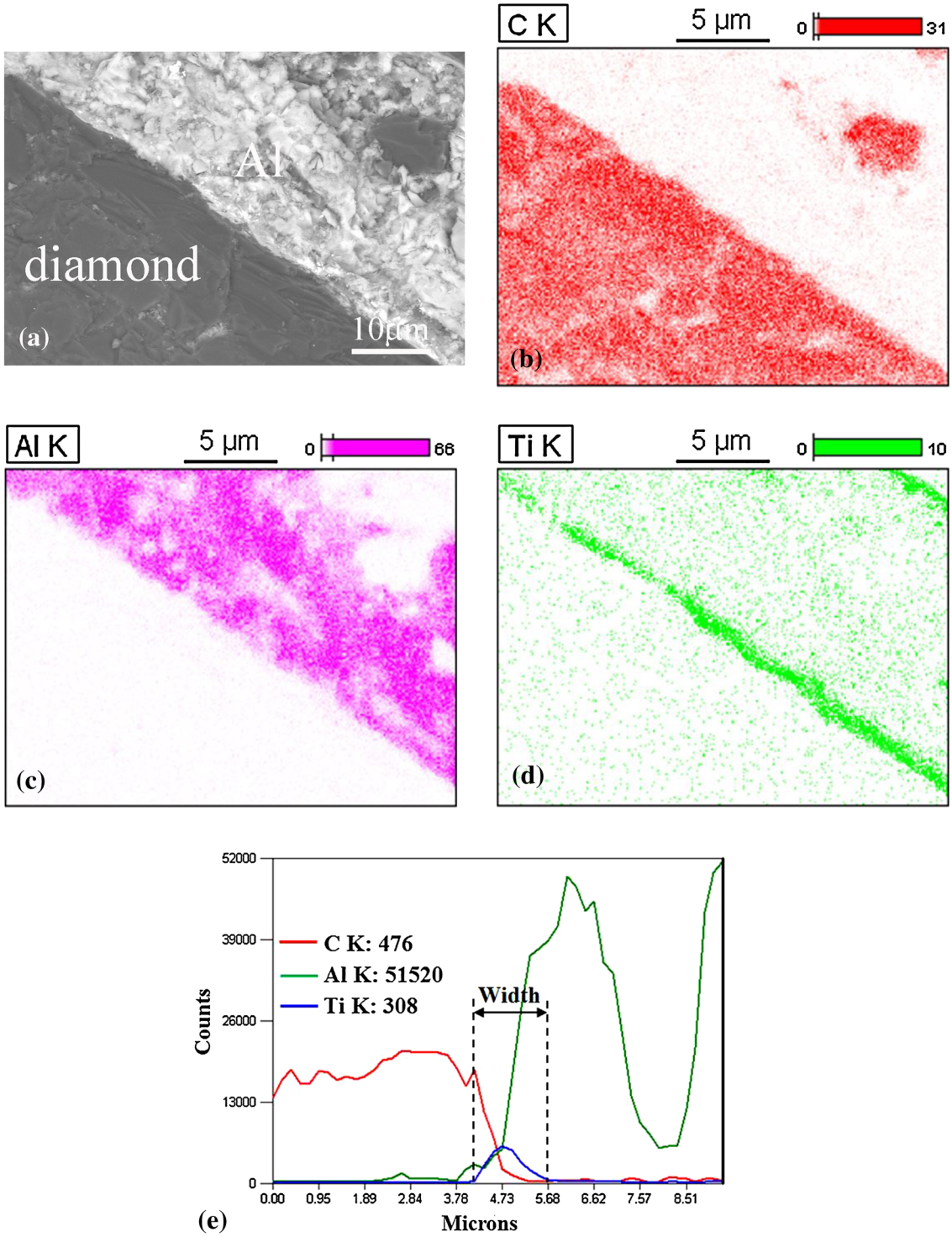

Fig. 3 EDS scan across an interface in (a) the Al-4.0 wt.% Ti/diamond composite: x-ray mapping of (b) C, (c) Al, and (d) Ti and (e) line scan of the elements

deformation because the measured E_0 values will be reduced with the development of defects in composites (Ref 8). The E_0 value was determined from the slope of the linear part from $\varepsilon = 0$ to 0.02%, and the results are given in Table 2. Generally, the measured E_0 value increased with increasing Ti content. This suggests that Ti alloying in Al matrix strengthens interfacial bonding in the Al-Ti/diamond composites. For comparison, the 265 GPa for the Al-2.0 wt.% Ti/diamond composite is lower than 333 GPa for the Al-2.0 wt.% Cu/diamond composite reported (Ref 7).

As summarized in Table 2, the tensile strength continually increased with increasing alloying Ti content, that is to say, with increasing the thickness of TiC layer. But too thick an interfacial layer will reduce the thermal conductivity of composite because TiC has a much lower thermal conductivity of 36.4 W/mK (Ref 16). For this consideration, alloying Ti

content was increased to a moderate level of 4.0 wt.% in this study.

3.2.2 Compressive Strength. Figure 5 shows the representative compressive stress-strain curves of the Al-Ti/diamond composites. As summarized in Table 2, the ultimate compressive strength of the composites increased monotonically up to 4.0 wt.% Ti. The strain at failure firstly increased to 1.0 wt.% Ti, before decreasing with further increasing Ti content. The results are consistent with the variation tendency of tensile strength.

3.2.3 Bending Strength. The bending stress-strain curves of the Al-Ti/diamond composites were not recorded. The ultimate bending strength was measured, as given in Table 2. Similar to tensile or compressive strength, the bending strength generally increased with increasing alloying Ti content. As mentioned above, this can be explained by both the alloy strengthening effect of Ti in Al matrix and the connection of interfacial TiC layer.

3.3 Fractography

Figure 6 shows the SEM observations of fractured surfaces of the Al-Ti/diamond composites. As shown in Fig. 6(a), besides many fractures observed in Al matrix, some diamond particles were also found to dispatch directly from Al matrix. It means that the Al/diamond interface could be weak. This explains partly why the tensile strength of the unmodified Al/diamond composite was the lowest among the composites. For the Al-4.0 wt.% Ti/diamond composite (Fig. 6b), the proportion of bare surfaces of diamond decreased dramatically, suggesting the enhancement of interfacial bonding between diamond and Al.

The dimples in Fig. 6(b) were found to be very small. In the Al-Ti/diamond composites, since the stage of plastic deformation in Al matrix is short, the dimples do not have enough time to coalesce before failure. This is supported by the tensile curves below 2.0 wt.% addition (Fig. 4).

4. Discussion

4.1 The Effect of Metal Matrix Alloying on Microstructure and Mechanical Properties of Al/Diamond Composites

The effect of metal matrix alloying on composite strength could be discussed from two aspects. First, a thicker TiC layer is beneficial to connecting diamond reinforcement and Al matrix. As shown in Fig. 4 and 5, the mechanical strength is enhanced by alloying Ti to Al matrix. The interfacial layer thickness increases with increasing alloying Ti content. As an example, Fig. 3 shows that an about 2-μm-thick interfacial layer is formed when 4.0 wt.% Ti is added to Al matrix. Second, Ti alloying plays a role in strengthening Al matrix. As shown in Table 3, with alloying 4.0 wt.% Ti to Al, the ultimate tensile strength of the Al-Ti alloy increased by a factor of more than two. While a portion of Ti alloying to Al matrix is consumed by the formation of TiC, which is verified by the XRD results in Fig. 1, the rest of Ti still remains and thus strengthens Al matrix.

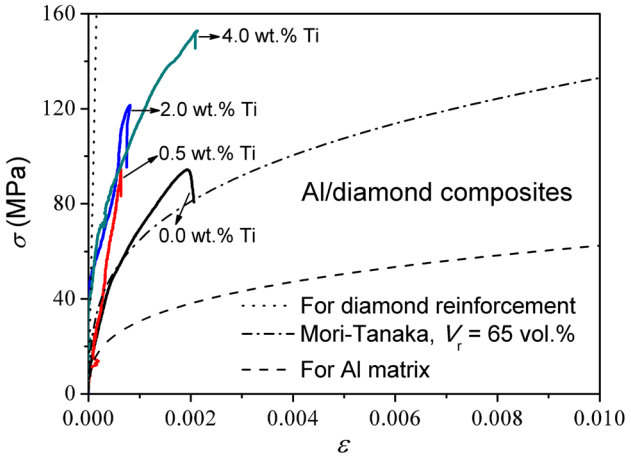

Fig. 4 Measured tensile stress-strain curves for the produced Al-Ti/diamond composites. Theoretical predictions of tensile stress-strain curves for Al-Ti/diamond composites, Al matrix, and diamond reinforcement are also shown. Hardening exponent of $n = 0.3$ is assumed in the predictions

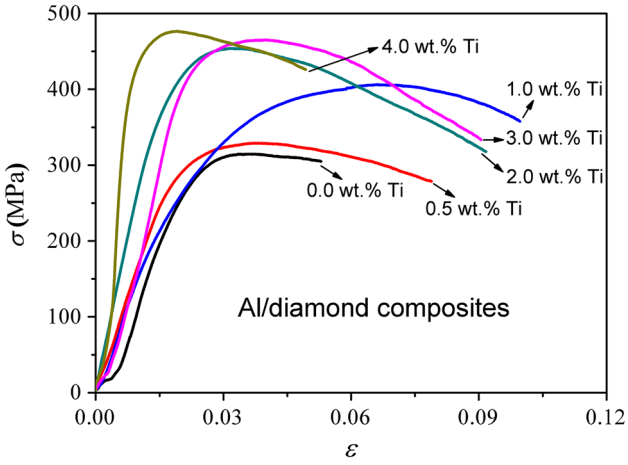

Fig. 5 Measured compressive stress-strain curves for the produced Al-Ti/diamond composites

Table 2 Measured mechanical strength for the produced Al-Ti/diamond composites

Alloying Ti content (wt.%)	0	0.5	1.0	2.0	3.0	4.0
Tensile yield stress $\sigma_{0.02\%}$, MPa	28	32	…	53	…	68
Tensile yield stress $\sigma_{0.2\%}$, MPa	92	…	…	…	…	149
Young's modulus E_0, GPa	140	160	…	265	…	340
Tensile strength σ_b, MPa	94 ± 5	95 ± 5	…	122 ± 4	…	153 ± 6
Compressive strength σ_{bc}, MPa	315 ± 9	329 ± 11	406 ± 13	454 ± 13	465 ± 15	477 ± 15
Bending strength σ_{bb}, MPa	273 ± 9	280 ± 7	322 ± 8	338 ± 10	361 ± 7	374 ± 11

The highest UTS value was obtained to be 153 MPa for the Al-4.0 wt.% Ti/diamond composite. The value is comparable to 155 MPa obtained for a Al-2.0 wt.% Cu/diamond composite (Ref 7), with the same diamond volume fraction of 65 vol.%. Nevertheless, the average particle size of diamond in this study is 159 μm that is much larger than 22 μm in literature (Ref 7). It is revealed that decreasing particulate reinforcement size will significantly enhance the mechanical properties of a composite (Ref 8). Accordingly, if smaller particle size of diamond is used, the tensile strength of the Al-Ti/diamond composites could be further enhanced. Therefore, one cannot make a reasonable comparison between the Al-2.0 wt.% Ti/diamond (UTS = 122 MPa) and the referenced Al-2.0 wt.% Cu/diamond (UTS = 155 MPa) due to a mixture of affecting factors of metallic matrix and diamond particle size. Currently, it is difficult to conclude which of the two Al alloy matrices is more efficient in enhancing the tensile strength of Al/diamond composites.

As summarized in Table 2, the mechanical strength of Al/diamond composites increases monotonically with increasing alloying Ti content up to 4.0 wt.%. It will be interesting to compare with the enhancement of thermal conductivity. Xue and Yu (Ref 11) reported that the thermal conductivity of Al-Ti/diamond composites increases with increasing alloying content up to 0.5 wt.% Ti, before decreasing with further increasing Ti content. Similarly, Weber and Tavangar (Ref 17) reported that, with increasing alloying element content, the thermal conductivity of both Cu-Cr/diamond and Cu-B/diamond composites increases to a critical alloying content (0.3 wt.% Cr or 0.2 wt.% B) and then begins to decrease. Since interfacial carbide layer usually has a low thermal conductivity, too thick a layer will hinder heat transport through interface. Therefore, there is a peak effect for the enhancement of thermal conductivity with increasing alloying element content. This finding reflects difference in heat transport and load transfer through an interface. It is clear that design guideline for thermal conducting composites will differ from that for mechanically reliable composites. To obtain metal/diamond composites with acceptable comprehensive performance for electronic packaging applications, a compromise between thermal conductivity and mechanical strength should be made when interfacial layer thickness is determined.

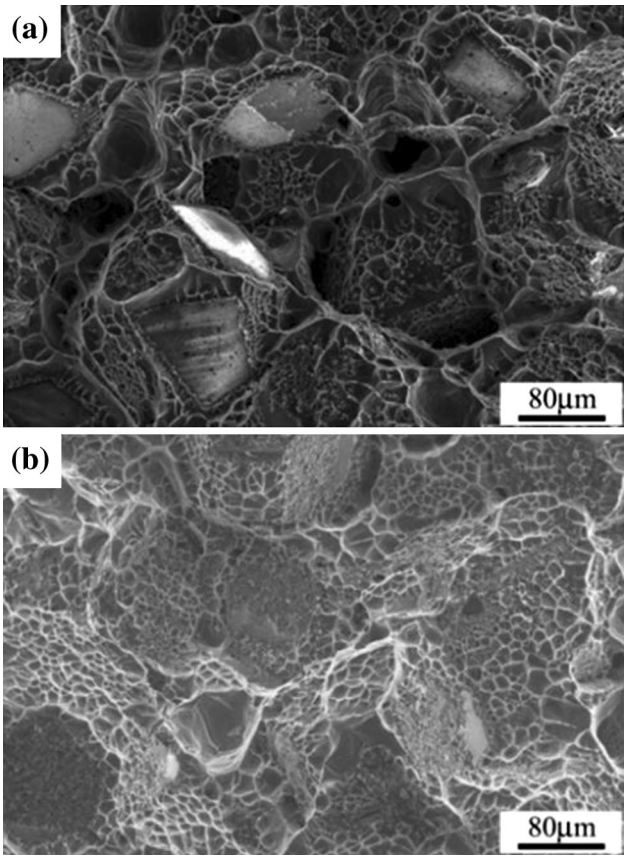

Fig. 6 SEM observations of fractured surfaces of the produced Al-Ti/diamond composites: (a) unmodified Al/diamond composite and (b) Al-4.0 wt.% Ti/diamond composite

4.2 The Correlation of Tensile Stress-Strain Curves of Al/Diamond Composites with Existing Model

Theoretical predictions of deformation of composites contribute to deep understanding of the underneath mechanism. Here, the Mori-Tanaka (Ref 18) model that deals with the elastic moduli of particulate-reinforced metal matrix composites is applied to correlate the tensile testing data. The formulation of effective moduli of composite is so complex that the derivation of analytical solution of tensile stress-strain constitutive equation is rather difficult and sometimes impossible. To solve this problem, we take advantage of Mueller and Mortensen's simplified formulations (Ref 19).

The material parameters involved in the analytical calculations for the Al/diamond composites were assumed to be K_m = 76 GPa, G_m = 26 GPa, and c = 250 MPa for Al matrix, and K_r = 443 GPa, G_r = 478 GPa (Ref 8), and V_r = 0.65 for diamond reinforcement. The hardening exponent n for Al matrix was assumed to be 0.3, a parameter reserved for metals. To assist in the evaluation of deformation behavior of Al/diamond composites, the elastic stress-strain curve of diamond reinforcement and strain-hardening curve of the Al matrix were also plotted. The Young's modulus was assumed to be 1055 GPa for diamond (Ref 8). By setting V_r = 0, the strain-hardening behavior of the Al matrix is separately outlined using the Mori-Tanaka model.

As shown in Fig. 4, all the measured data are located between the elastic stress-strain curve for diamond reinforcement and the strain-hardening curve for the Al matrix. This is justified because the deformation of a composite is a combination of the constituents. The Mori-Tanaka model is capable of predicting moduli of composites containing high volume fraction of spherical inclusions (Ref 18). Since 65 vol.% reinforcement of diamond was used, the model is suitable for predicting the deformation of the Al/diamond composites. As

Table 3 Measured tensile strength for the Al-Ti alloys used as metal matrix

Alloying Ti content, wt.%	0	0.5	2.0	4.0
Tensile strength σ_b, MPa	40 ± 5	65 ± 5	74 ± 4	106 ± 5

seen in Fig. 4, the Mori-Tanaka model predicts the lowest flow stress since the moduli predicted by the model correspond to the Hashin-Shtrikman lower bound if the matrix is soft phase, just like Al matrix in this study.

5. Conclusions

(1) Ti alloying to Al matrix can create interfacial TiC layer in the Al/diamond composites produced by gas pressure infiltration. An interfacial layer of about 2 μm thickness was formed between Al and diamond at 4.0 wt.% Ti addition.
(2) The tensile, compressive, and bending strength of the Al-Ti/diamond composites increases monotonically with increasing alloying Ti content. Both the interfacial layer and matrix strengthening play a critical role in enhancing the mechanical strength of the composites.
(3) The produced Al-4.0 wt.% Ti/diamond composite exhibited a high tensile strength of 153 MPa but a small strain at failure of 0.2%.

Acknowledgments

This work is financially supported by the National Natural Science Foundation of China (51271017) and International Science and Technology Cooperation Program of China (2014DFA51610). Fruitful discussion with Prof. Yandong Wang is appreciated.

References

1. M.A. Stubblefield, S.S. Pang, and V.A. Cundy, Heat Loss in Insulated Pipe the Influence of Thermal Contact Resistance: A Case Study, *Compos. Part B*, 1996, **27**, p 85–93
2. S. Wang and J. Qiu, Enhancing Thermal Conductivity of Glass Fiber/Polymer Composites Through Carbon Nanotubes Incorporation, *Compos. Part B*, 2010, **41**, p 533–536
3. K. Loutfy, H. Hirotsuru, Advanced Diamond Based Metal Matrix Composites for Thermal Management of RF Devices, *IEEE 12th Annual Wireless and Microwave Technology Conference*, 2011, p 1–5
4. Z.Q. Tan, Z.Q. Li, G.L. Fan, X.Z. Kai, G. Ji, L.T. Zhang, and D. Zhang, Fabrication of Diamond/Aluminum Composites by Vacuum Hot Pressing: Process Optimization and Thermal Properties, *Compos. Part B*, 2013, **47**, p 173–180
5. K. Mizuuchi, K. Inoue, Y. Agari, Y. Morisada, M. Sugioka, M. Tanaka, T. Takeuchi, J. Tani, M. Kawahara, and Y. Makino, Processing of Diamond Particle Dispersed Aluminum Matrix Composites in Continuous Solid-Liquid Co-existent State by SPS and Their Thermal Properties, *Compos. Part B*, 2011, **42**, p 825–831
6. L. Weber and R. Tavangar, Diamond-Based Metal Matrix Composites for Thermal Management Made by Liquid Metal Infiltration—Potential and Limits, *Adv. Mater. Res.*, 2009, **59**, p 111–115
7. K.A. Weidenmann, R. Tavangar, and L. Weber, Rigidity of Diamond Reinforced Metals Featuring High Particle Contents, *Compos. Sci. Technol.*, 2009, **69**, p 1660–1666
8. K.A. Weidenmann, R. Tavangar, and L. Weber, Mechanical Behaviour of Diamond Reinforced Metals, *Mater. Sci. Eng. A*, 2009, **523**, p 226–234
9. Y. Zhang, X.T. Wang, S.B. Jiang, and J.H. Wu, Thermo-Physical Properties of Ti-Coated Diamond/Al Composites Prepared by Pressure Infiltration, *Mater. Sci. Forum*, 2010, **654–656**, p 2572–2575
10. X.B. Liang, C.C. Jia, K. Chu, H. Chen, J.H. Nie, and W.J. Gao, Thermal Conductivity and Microstructure of Al/Diamond Composites with Ti-Coated Diamond Particles Consolidated by Spark Plasma Sintering, *J. Compos. Mater.*, 2012, **46**, p 1127–1136
11. C. Xue and J.K. Yu, Enhanced Thermal Conductivity in Diamond/Aluminum Composites: Comparison Between the Methods of Adding Ti into Al Matrix and Coating Ti onto Diamond Surface, *Surf. Coat. Technol.*, 2013, **17**, p 46–50
12. H. Feng, J.K. Yu, and W. Tan, Microstructure and Thermal Properties of Diamond/Aluminum Composites with TiC Coating on Diamond Particles, *Mater. Chem. Phys.*, 2010, **124**, p 851–855
13. O. Beffort, F.A. Khalid, L. Weber, P. Ruch, U.E. Klotz, S. Meier, and S. Kleiner, Interface Formation in Infiltrated Al(Si)/Diamond Composites, *Diam. Relat. Mater.*, 2006, **15**, p 1250–1260
14. J.H. Wu, H.L. Zhang, Y. Zhang, J.W. Li, and X.T. Wang, The Role of Ti Coating in Enhancing Tensile Strength of Al/Diamond Composites, *Mater. Sci. Eng. A*, 2013, **565**, p 33–37
15. M. Kouzeli and A. Mortensen, Size Dependent Strengthening in Particle Reinforced Aluminium, *Acta Mater.*, 2002, **50**, p 39–51
16. Y. Zhang, H.L. Zhang, J.H. Wu, and X.T. Wang, Enhanced Thermal Conductivity in Copper Matrix Composites Reinforced with Titanium-Coated Diamond Particles, *Scr. Mater.*, 2011, **65**, p 1097–1100
17. L. Weber and R. Tavangar, On the Influence of Active Element Content on the Thermal Conductivity and Thermal Expansion of Cu-X (X = Cr, B) Diamond Composites, *Scr. Mater.*, 2007, **57**, p 988–991
18. T. Mori and K. Tanaka, Average Stress in Matrix and Average Elastic Energy of Materials with Misfitting Inclusions, *Acta Metall.*, 1973, **21**, p 571–574
19. R. Mueller and A. Mortensen, Simplified Prediction of the Monotonic Uniaxial Stress-Strain Curve of Non-linear Particulate Composites, *Acta Mater.*, 2006, **54**, p 2145–2155